

High-temperature-resistant chemical composition Bragg gratings in Er³⁺-doped optical fiber

S. Trpkovski, D. J. Kitcher, G. W. Baxter, and S. F. Collins

Optical Technology Research Laboratory, Victoria University, P.O. Box 14428, Melbourne, Victoria 8001, Australia

S. A. Wade

Department of Mechanical Engineering, Monash University, Victoria 3800, Australia

Received October 7, 2004

Chemical composition gratings (CCGs), unlike standard fiber Bragg gratings (FBGs), do not suffer a significant decrease in reflectance or an irreversible wavelength shift when they are exposed to elevated temperatures. To date, the growth of CCGs has been related to the fluorine content of the fibers in which they are written. It is shown that FBGs with high thermal stability, resembling CCGs, can be fabricated in Er³⁺-doped optical fibers that do not contain any fluorine. © 2005 Optical Society of America

OCIS codes: 060.2370, 230.1480, 060.2290, 060.2410.

The application of fiber Bragg gratings (FBGs) for the measurement of both temperature and strain is attractive because the wavelength-encoded signal is unaffected by intensity variations in either the light source or the fiber path.^{1,2} The usefulness of FBGs in standard communications fiber for measurement at elevated temperatures, however, is severely restricted, since the reflectance tends to decrease.³ Generally the reflectance of type I FBGs written in standard telecommunications-grade fiber starts to drop, and the Bragg wavelength experiences an irreversible shift toward shorter wavelengths, when the grating is subjected to temperatures above ~100°C.⁴ The decay of FBGs in a range of fibers, particularly for characterization of their longevity by accelerated aging has been studied extensively,^{4,5} to provide predictions of the grating lifetime at particular temperatures.

The most important determinants of grating survivability at elevated temperatures are the grating type, the fiber composition, and the possible use of hydrogen loading. Type II gratings written with a single high-power pulse are able to remain operable at temperatures as high as 800°C but at the expense of inducing damage tracks in the optical fiber.⁶ Similarly, type IIA gratings written in Ge-Si and B-Ge-Si fibers exhibited greater thermal stability than type I gratings.⁷ A variety of fiber compositions have been characterized in terms of how the Bragg reflectance of FBGs inscribed in them survive when subjected to an isochronal heating process at various temperatures. For example, the aforementioned Ge-Si fibers,⁷ with either type I or type IIA gratings survived up to ~750°C but with low grating strengths compared with the B-Ge-Si fibers, in which both type I and type IIA gratings were inscribed that were almost erased by 350 and 500°C, respectively. The addition of tin (Sn) to Ge-Si fiber enhanced FBG stability compared with Ge-Si and B-Ge-Si fibers, with Sn-Ge-Si fibers surviving temperatures close to

800°C but with relatively low reflectance.⁸ Similarly, gratings inscribed in hydrogen-loaded telecommunications fiber and borogermanosilicate fiber were erased when exposed to temperatures less than 500°C, whereas those in tin silicate fiber survived up to near 800°C.³

Gratings with superior high-temperature stability referred to as chemical composition gratings (CCGs) have been reported.⁹⁻¹¹ It has been proposed that UV-induced chemical reactions result in the formation of certain molecules that subsequently diffuse out of the UV-exposed regions of the core while the fiber is subjected to high-temperature heat treatment. The consequential variation of chemical composition along the fiber core results in a corresponding refractive-index modulation and hence a Bragg grating. These CCGs in Ge-F-Si-doped fiber remain stable at temperatures up to 1000°C.⁹ They are fabricated by inscribing a standard type I FBG in a hydrogen-loaded sample of this fiber and then subjecting the FBG to very high temperatures (>800°C) for an extended period of time (>1 h).¹⁰ During this time the initial type I Bragg grating disappears and subsequently a CCG appears. Studies of the decay of these gratings above 1000°C reveal how the grating decay increases with temperature and support the proposition that this decay is associated with the diffusion of fluorine compounds.¹¹

For the work discussed in this Letter two different Er³⁺-doped fibers were used (denoted as Er1 and Er2), as detailed in Table 1, neither of which contained fluorine. The fibers were fabricated at the University of Nice (Nice, France) by use of a modified chemical-vapor-deposition technique with solution doping. Type I FBGs were fabricated by use of a frequency-doubled cw argon-ion laser operating at 244 nm and a phase mask that produced a Bragg wavelength of ~1540 nm. Table 1 also summarizes the hydrogen loading, FBG writing conditions, and characteristics of each fiber. Short lengths (~10 cm)

Table 1. Characteristics of the Two Er-doped Fibers Used and the Type I FBGs Inscribed Within

Fiber Designation	Er1	Er2
Core composition	Si-Ge-P ₂ O ₅ -Al	Si-Ge-Sn
Fiber cutoff wavelength (nm)	~1530	~1410
Core/cladding diameters (μm)	8/125	5/125
Er ³⁺ -dopant concentration (parts in 10 ⁶)	~1400	~100
Hydrogen-loading Pressure (atm)	80	123
Temperature ($^{\circ}\text{C}$)	80	55
Duration (h)	168	168
UV power density on the fiber (W/cm^2)	~4	~25
UV exposure time (min)	9	1 (scanning mode)
Grating Reflectivity (%)	~90	~95
Length (mm)	10	2

of Er³⁺-doped fiber, in which FBGs were inscribed, were spliced between longer lengths of Corning SMF28 telecommunications fiber, to allow real-time monitoring of the FBG transmission spectra during the writing and annealing processes.

The transmitted spectral profile of the Bragg grating was monitored with an optical spectrum analyzer (0.05-nm resolution) with illumination provided by a broadband 1550-nm superluminescent LED source. The fiber containing the FBG was passed through a tube oven, and a K-type thermocouple was placed alongside the FBG for measurement of the temperature during the tests. The fiber was clamped at either end, allowing it to be suspended in the tube oven to prevent the FBG from touching any other surface during the annealing process. A LabVIEW-based program recorded FBG spectra at set intervals during the testing procedure.

To measure the thermal stability of the Bragg reflectance, an initial isochronal annealing test was performed on a FBG in an Er1 (Er1-a) fiber sample at 24-h intervals. At each of these intervals as shown in Fig. 1, isothermal annealing was performed at steps of 100 $^{\circ}\text{C}$ from 100 to 800 $^{\circ}\text{C}$. As shown in Fig. 1, during the 800 $^{\circ}\text{C}$ step the type I grating experienced complete erasure. Subsequently, however, a new grating began to develop in a fashion that resembled the growth characteristic of a CCG.⁹ Unfortunately, observation of the growth process of the newly formed grating was interrupted when it had reached a reflectance of approximately 20% because of a sudden, unexplained total loss of signal. The observed grating decay at each temperature shown in Fig. 1, which indicates that the FBG experienced an initial fast decay followed by a subsequent slow decay, is typical of a type I FBG.⁵ The subsequent growth of another grating after a period of ~2 h resembled behavior similar to that observed in Ge-F-Si-doped fiber.

Three similar tests were conducted in other Er1 and Er2 fiber samples, and the growth dynamics of the newly formed Bragg gratings is evident in Fig. 2. No degradation in the propagating signal was observed in these samples as was experienced with the first sample (Er1-a). In each case a slightly different annealing procedure was used to see if the details of the annealing process affected the spectral properties of the newly formed Bragg grating. The second Er1

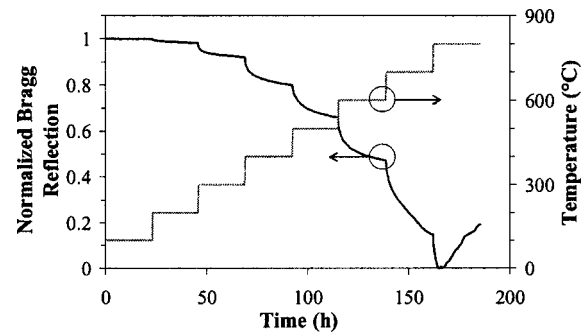


Fig. 1. Grating reflectivity in sample Er1-a during the heating process, showing the erasure of the type I grating and the subsequent growth of a newly formed grating.

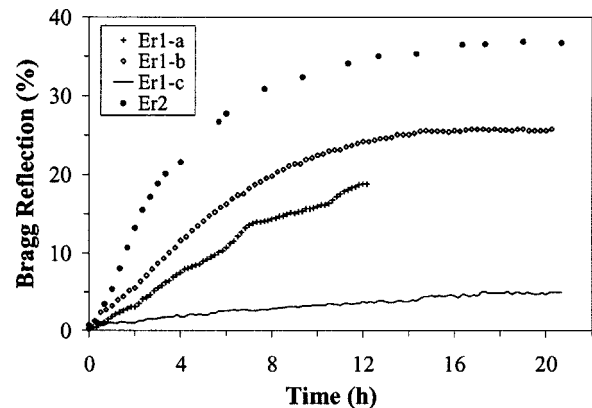


Fig. 2. Growth of newly formed gratings in Er1 and Er2 fiber at 800 $^{\circ}\text{C}$.

sample (Er1-b) was preannealed for 24 h at 700 $^{\circ}\text{C}$ before being exposed to 800 $^{\circ}\text{C}$. The third sample (Er1-c) was directly exposed to 800 $^{\circ}\text{C}$, while the Er2 sample was isochronally preannealed at 600 and 700 $^{\circ}\text{C}$ for 24 h before being exposed to 800 $^{\circ}\text{C}$.

The investigation of the dependence of the newly formed gratings to various annealing processes depicted in Fig. 2 indicates a correlation between the annealing process and the resultant reflectivity that can be achieved with the newly formed Bragg gratings in the Er1 fiber. In particular, exposing the Er1-b sample to an additional isothermal step of 700 $^{\circ}\text{C}$ for 24 h resulted in an approximate fivefold increase in reflectance of the newly formed Bragg

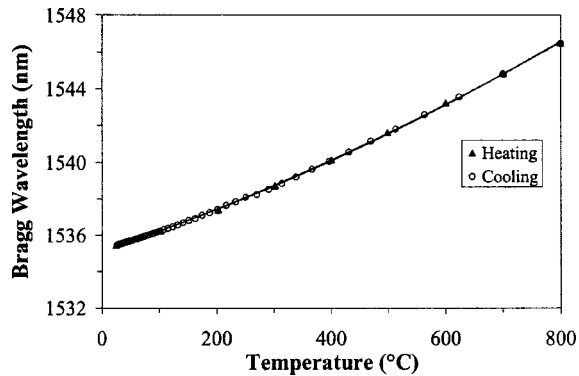


Fig. 3. Temperature dependence of a newly formed grating in Er1-b fiber. The solid curve represents a quadratic fit.

grating. Grating growth in Er1-a appeared to be at a slower rate relative to the Er1-b but appeared to still be growing when the test was interrupted. The Bragg grating formed in the Er2 sample exhibited the largest reflectance. Although it has been shown that additional annealing steps increase the final reflectance of CCGs,¹² further tests are required before any conclusions can be drawn as to whether this increase in reflectance was due to the additional annealing step or to the different fiber composition than that of Er1. Other variables that may affect the final Bragg grating strength are the different laser source, hydrogen-loading conditions, and the initial type I grating strength. It was noted that the newly formed Bragg gratings exhibited a decrease of their Bragg wavelength of ~ 0.7 nm compared with their initial type I Bragg wavelengths at room temperature. This decrease is in contrast to standard FBGs and suggests that the average refractive-index modulation experiences a decrease rather than the usual increase.

The ongoing repeatability and stability of the newly formed grating was investigated by temperature cycling a Er1-b sample from room temperature to 800°C. The results shown in Fig. 3 for the temperature calibration indicate that any hysteresis in the response of the newly formed Bragg grating is negligible. Figure 3 also shows how the dependence of the Bragg wavelength on temperature departs from linearity over a wide temperature range, an effect that was previously noted in standard FBGs¹³ and in other FBG samples in Er2 fiber.¹⁴ The solid curve in Fig. 3 is best explained by the following quadratic equation:

$$\lambda_B = 4.967 \times 10^{-6} T^2 + 1.029 \times 10^{-2} T + 1535.171,$$

where the Bragg wavelength λ_B is measured in nanometers and the temperature T is given in degrees Celsius. The quadratic that was fitted to the data resulted in an R^2 value of 0.9998. For sensing applications the Bragg gratings' temperature accuracy was also assessed. The root-mean-square error was found

to be 3.4°C, which may be interpreted as a temperature accuracy of 0.4% over the temperature range indicated in Fig. 3.

In conclusion, FBGs resembling CCGs, having reflectivities of up to 35%, have been fabricated in Er³⁺-doped optical fiber that did not contain fluorine. The FBGs obtained in these preliminary measurements demonstrated very good thermal stability to temperatures up to 800°C, with no sign of a reduction in reflectance or of an irreversible shift of the Bragg wavelength. That this is so suggests that these FBGs could be useful for high-temperature applications. Ongoing work is being performed to determine the chemical processes involved in the formation of these FBGs. This would aid in the optimization of the spectral properties of these FBGs.

The authors acknowledge the use of the FigFab facility, maintained by Swinburne University of Technology, the Defence Science and Technology Organization, and Monash University, to write some of the FBGs used in this work and thank the Australian Research Council for financial support. We also thank Thanh Nguyen and the Laboratoire de Physique de la Matière Condensée, France, for providing one of the rare-earth-doped fibers that was used.

The authors may be contacted at stephen.collins@vu.edu.au.

References

1. A. Othonos and K. Kalli, *Fiber Bragg Gratings* (Artech House, Norwood, Mass., 1999).
2. Y. J. Rao, *Opt. Lasers Eng.* **31**, 297 (1999).
3. G. Brambilla and V. Pruneri, *IEEE J. Sel. Top. Quantum Electron.* **7**, 403 (2001).
4. S. Pal, J. Mandal, T. Sun, and K. T. V. Grattan, *Appl. Opt.* **42**, 2188 (2003).
5. T. Erdogan, V. Mizrahi, P. J. Lemaire, and D. Monroe, *J. Appl. Phys.* **76**, 73 (1994).
6. J. L. Archambault, L. Reekie, and P. St. J. Russell, *Electron. Lett.* **29**, 453 (1993).
7. S. Pal, J. Mandal, T. Sun, K. T. V. Grattan, M. Fokine, F. Carlsson, P. Y. Fonjallaz, S. A. Wade, and S. F. Collins, *Meas. Sci. Technol.* **14**, 1131 (2003).
8. L. Dong, J. L. Cruz, L. Reekie, M. G. Xu, and D. N. Payne, *IEEE Photon. Technol. Lett.* **7**, 1048 (1995).
9. M. Fokine, B. E. Sahlgren, and R. Stubbe, in *Bragg Gratings, Photosensitivity, and Poling in Glass Fibers and Waveguides: Applications and Fundamentals*, Vol. 7 of OSA Technical Digest Series (Optical Society of America, Washington, D.C., 1997), pp. 58–60.
10. M. Fokine, *J. Opt. Soc. Am. B* **19**, 1759 (2002).
11. M. Fokine, *Opt. Lett.* **27**, 1016 (2002).
12. M. Fokine, *Opt. Lett.* **27**, 1974 (2002).
13. G. M. H. Flockhart, W. N. MacPherson, J. S. Barton, J. D. C. Jones, L. Zhang, and I. Bennion, in *Technical Digest of the 15th International Conference on Optical Fiber Sensors*, E. Udd, ed. (IEEE, Piscataway, N.J., 2002), pp. 75–78.
14. S. Pal, T. Sun, K. T. V. Grattan, S. A. Wade, S. F. Collins, G. W. Baxter, B. Dussardier, and G. Monnom, *J. Opt. Soc. Am. A* **21**, 1503 (2004).